



1     **Dust Opacities inside Dust Devil Column in the Taklimakan Desert**

2     Zhaopeng Luan<sup>1,2,3</sup>, Yongxiang Han<sup>1,2</sup>, Feng Liu<sup>1,2</sup>, Tianliang Zhao<sup>1,2</sup>, Chong Liu<sup>1,2</sup>,

3                     Mark J. Rood<sup>4</sup>, Xinghua Yang<sup>5</sup>, Qing He<sup>5</sup>, Huichao Lu<sup>3</sup>

4     <sup>1</sup> Collaborative Innovation Center on Forecast and Evaluation of Meteorological Disasters,

5     Nanjing University of Information Science and Technology, Nanjing, 210044, China

6     <sup>2</sup> Key Laboratory for Aerosol-Cloud-Precipitation of China Meteorological Administration,

7     Nanjing University of Information Science and Technology, Nanjing, 210044, China

8     <sup>3</sup> Tai'an Meteorological Bureau, Tai'an, 271000, China

9     <sup>4</sup> Department of Civil & Environmental Engineering, University of Illinois at Urbana-Champaign,

10     Illinois, 61820, USA

11     <sup>5</sup> Institute of Desert Meteorology, China Meteorological Administration, Urumqi, 830002, China

12     Correspondence to: Tianliang Zhao (tlzhao@nuist.edu.cn)

13     **Abstract.** The distribution of particulate matter (dust) in dust devils (DDs), which are  
14     well-defined vortexes of wind that range from 1 m to 1,000 m tall, is quantitatively  
15     quantified here based on light transmission. We applied the Digital Optical Method  
16     (DOM) with digital still cameras to quantify the opacity of the DDs in the Taklimakan  
17     Desert, China. This study presents the following unique and important results and  
18     interpretations: 1) the distinct horizontal distributions of opacity indirectly proved the  
19     existence of DDs' zone of weak winds in the center of the swirling vortex, similar like  
20     the eye of tropical cyclone, which is difficult to be observed directly; 2) The opacity  
21     of the DDs decreases with increasing height, however, the dust does appears to settle  
22     out, and the relatively calm eye leads to a minimum in dust opacity at the eye; 3) The



1 horizontal distribution of opacity is quasi symmetric with a bimodal across the eye of  
2 the DDs; and 4) A new robust method is developed for the representation of  
3 three-dimensional structure of opacity based on the observed two-dimensional  
4 structures provided by DOM. This research not only proposes a highly reliable, low  
5 cost and efficient methodology to characterize the inside structure of DDs, but also  
6 provides the information on estimation of dust emissions caused by DDs.

7 **Keywords:** dust devil; digital optical; opacity; dust devil eye; 3-D structure

8

## 9 **1 Introduction**

10 Well-defined vortexes of wind that range from 1 m to 1,000 m tall, also known as  
11 dust devils (DDs) are the most common small scale (< 50 m diameter at ground level)  
12 dust transmitting system in the atmosphere(Kanak, 2005;Kanak et al., 2000;Leovy,  
13 2003). It is a special case of columnar, ground-based convective vortex occurring in  
14 the lower atmospheric boundary layer (Gu et al., 2008;Koch and Renno, 2005).  
15 Occurrences of wind devils are associated with weak wind, sunny weather, and local  
16 surface pressure fluctuations which are dominated by heterogeneous solar radiation  
17 due to uneven heating of the ground, that leads to a rising convection vortex rotation  
18 containing particulate matter (PM, dust) under certain conditions of angular  
19 momentum(Duan et al., 2013).The theory and numerical model results suggest that  
20 DDs have significant potential for high dust loadings. DDs contribute to one third of  
21 the total natural particulate mass emitted to the atmosphere annually (Koch and Renno,  
22 2005). Emissions of total primary particulate mass by DDs to the atmosphere is as



1 high as 65% in the United States (Gillette and Sinclair, 1990). About 77%-87% of the  
2 primary particulate mass emitted to the atmosphere in Chinese deserts is caused by  
3 DDs (Han et al., 2008;Deng et al., 2011;Zhang et al., 1994), while DDs generate 30%  
4 of the primary particulate mass emitted to the atmosphere in the Sahara Desert  
5 (Marsham et al., 2008). These results imply that DDs may play an equal or more  
6 important role than sandstorms when considering the total emissions of PM into the  
7 atmosphere. DDs affect not only air quality of arid areas but also impact global or  
8 regional climate through the “umbrella” (Wei et al., 1998) and “condensation nucleus”  
9 effects (Wang and Zhang, 2001) in the atmosphere as well as the “iron fertilizer effect”  
10 in open oceans (Han et al., 2006) that occur because of the remote entrainment,  
11 transmission and then deposition of dust from the atmosphere.

12 However, physical processes and mechanisms of dust entrainment by DDs are  
13 poorly understood. It is extremely difficult to observe DDs because of their sporadic  
14 and unpredictable mobile paths. So the basic structure and characteristic parameters  
15 have long been based on human observations by Ives (1947) and Sinclair (1964). DDs’  
16 central core structure has been remarkably observed with mobile Doppler radar  
17 (Bluestein et al., 2004) and their center pressure has been characterized by pressure  
18 logger (Lorenz, 2012;Lorenz, 2013). However, data obtained from the mobile  
19 Doppler radar and pressure logger depend on locating the instruments along the  
20 estimated path of the DDs where they may appear, and the measurements are mainly  
21 focused on meteorological parameters. The high-cost measurement implementation  
22 requires extensive and expensive resources. In addition, LES (Large Eddy Simulation)



1 have also been applied to DD studies by Toigo (2003), Ito et al.(2010) and Kanak et al.  
2 (2000; 2005). The condition of weaker wind and stronger surface heat flux favorable  
3 for the formation of dust devil is confirmed according to theirs studies. Gu et al. (2003;  
4 2010) even provided the meteorological characteristics inside of DDs by numerical  
5 simulation. However, field observations of DDs to compare to and validate the  
6 modeled results including vortex dynamics are critical and necessary (Leovy, 2003).

7 The Digital Optical Method (DOM) was developed to measure opacities of plumes  
8 in the atmosphere emitted from stationary point sources (Du et al., 2007; Du et al.,  
9 2009). DOM uses a digital still camera and software for processing the digital pictures  
10 to determine plume opacity. This method was also used to quantify plume opacities  
11 for fugitive dust plumes in the atmosphere (Du et al., 2013). DOM was developed to  
12 quantify plume opacity at low cost, easy implementation, with improved accuracy  
13 compared to human observations of plume opacity, and to provide digital record.

14 We conducted a DD field campaign in the Taklimakan Desert, the largest desert in  
15 China and the world's second largest liquidity desert during July 2014. This is the first  
16 time to use DOM to observe DDs. Two dimensional (2D) structures of dust devils are  
17 archived with the digital images of the DD and processing with DOM software. This  
18 effort provides horizontal and vertical distributions of opacity values in DDs, and  
19 presents the first three-dimensional (3D) opacity structure of DDs. It is important to  
20 quantify the structure which is helpful to estimate dust emissions of DDs. The study  
21 thus services to provide insightful information for DD numerical simulation and  
22 validation.



1

## 2 **2 Methods**

### 3 *2.1 Image acquisition and processing*

4     The observational investigation site is located in the Xiaotang region (40°50'N,  
5     84°10'E, altitude 943.9m), in the hinterland location of the Taklimakan Desert (see  
6     Fig.1). Xiaotang is a typical desert-Gobi transitional zone where DDs occur  
7     frequently according to local meteorological observations. During the observations  
8     from 2 to 14 July, 2014 digital images were obtained with two digital still cameras  
9     (Sony Cyber-shot Model DSC-P100). In order to obtain the appropriate background  
10    for taking the pictures, the camera is back to the sun within a 140° sector (ASTM  
11    D-7520). All pictures archived as JPEG files. Most observed DDs show inverted  
12    circular cone and are quasi-symmetric shape across the DD's eye with a height of  
13    several tens to hundreds meters. None of the DDs have absolute symmetry due to the  
14    heterogeneous distribution of dust particles in the DD caused by the time-dependent  
15    dynamics.

16    A digital image of a typical DD is illustrated in Fig.1 to describe how to determine  
17    the DD opacity values. The vertical curved lines were added to the image to represent  
18    auxiliary lines describing vertical grids for estimation of opacity values. The sky  
19    background of the DD is relatively uniform as shown in Fig.1. The upright electric  
20    pole right next to the DD with a height of 4.5 m was a reference to measure the height  
21    and diameter of the DDs. The DD with a base radius of 6.4 m and a height of 23.0 m  
22    has a maximum diameter of 15.8 m at the height of 16.0 m. In order to examine the



1 spatial distribution of dust concentration within the DD's dust cone, we horizontally  
2 set the cone into 0.4 m grids with 15 auxiliary upward lines parallel to the DD's  
3 conical surface. The centerline (line 0) is a vertical line from the bottom of the DD's  
4 eye. For the sake of clarity, we count lines on the left of the centerline from 1 to 7,  
5 while denoting lines to the right of the center as A to H (Fig.1b).

## 6 *2.2 Calculation of opacity*

7 DOM's transmission model was used in this study due to the uniform background  
8 sky conditions (e.g., uniform clear or overcast sky) for the DDs. And the challenge to  
9 install contrasting backgrounds behind and next to the DDs as needed with DOM's  
10 contrast model (Du et al., 2007). The transmission model determines the plume's  
11 opacity based on the radiance from the plume and the radiance from the plume's  
12 background. Part of the radiance ( $N_0$ ) from the sky is lost as it passes through the  
13 plume due to light scattering and/or absorption.  $N$  denotes the radiances received by  
14 the charge-coupled device (CCD) of the digital camera that correspond to the sky  
15 background, in terms of pixel values:

$$16 \quad N = N_0 T_0 + N^*$$

17  $T_0$  denotes the transmittance of the plume-free atmosphere along the path between the  
18 camera and the sky background.  $N^*$  is the path radiance of the atmosphere along the  
19 same path, which is from direct, diffuse, and reflected radiances scattered into the  
20 sight path by ambient air and aerosols (Du et al., 2013), and can be estimated with an  
21 equilibrium radiance model for uniform illumination and negligible absorption:

$$22 \quad N^* = N_0(1 - T_0)$$



1 From the two equation, getting the results of  $N=N_0$ .

2 Therefore, when the radiance reaches the camera ( $N_p$ ), it is caused by the attenuated  
3 radiance value from the plume ( $N_{T1}$ ), diffusive radiance value ( $N_{T2}$ ), and attenuation  
4 of the radiance caused by the surrounding atmosphere (which is negligible compared  
5 to the DD). The attenuated radiance value ( $N_{T1}$ ) results from  $N_0$  after the light is  
6 scattered and/or absorbed by the plume and the diffusive radiance value ( $N_{T2}$ ) is  
7 caused by other sources of light than the uniform sky background (Fig.2). According  
8 to the definition of opacity:

$$9 \quad \text{Opacity} = 1 - \frac{N_{t1}}{N_0} = 1 - \frac{N_p - N_{t2}}{N}$$

10 Because the camera did not directly measure  $N_{t2}$ , the proportionality coefficient,  $K$ , is  
11 defined by  $N_{t2} = K \cdot N \cdot \text{Opacity}$  (Du et al., 2007), and then the plume opacity could be  
12 determined by the transmission model as described by:

$$13 \quad \text{Opacity} = \frac{1 - \frac{N_p}{N}}{1 - K}$$

14  $N_p$  is the equivalent radiance value recorded by the camera, in terms of pixel values,  
15 caused by radiance from the plume ( $N_T$ ) and path radiance of the atmosphere.  $N$  is the  
16 equivalent radiance value recorded by the camera, in terms of pixel values, after  $N_0$   
17 passes through the DD-free atmosphere.  $K$  value of 1.4 in the transmission model is  
18 used.

### 19 **3 Results and discussion**

#### 20 *3.1 The vertical profile of opacity*

21 Fig. 3a, b, and c demonstrate the opacity profiles of the vertical grid lines, as shown



1 in Fig.1. It can be seen that: 1) The opacity profiles are non-uniform distributions in  
2 the vertical direction, and the vertical variation of opacity becomes more significant  
3 from the inner to the outer portions of the conical dust plume (See from the both  
4 Fig.3a and b), 2) The opacity profiles from center to both sides show quasi-symmetry  
5 but none of them are absolutely symmetrical; and 3) The opacity values generally  
6 decrease with height. However, the opacity decreases more rapidly at lower levels  
7 than upper ones. The averaged lapse rate (percent change in opacity values with  
8 increasing height) for the profile is 4.1% per meter below 10 m height over which the  
9 lapse rate drops to 0.6% per meter (Fig.3c).

### 10 *3.2 The horizontal variation of opacity*

11 From the horizontal variation of the opacity at different levels, it is observed that: 1)  
12 the horizontal opacity values increase first and then decrease from the center part to  
13 both sides at the base of the DD, implying that the DD is quasi-symmetric; 2) The  
14 opacity caused by dust aerosols and the corresponding dust concentrations are  
15 decreasing with height within the DD, and the opacity is a monotonically decreasing  
16 function as height increase. The maximum opacity is observed at the bottom of the  
17 DD (Fig. 4a); and 3) on the right side of the DD, the magnitude of opacity is greater  
18 than the left side (Fig.4). Therefore DOM method is able to capture all important  
19 well-known natures of DD including non-absolute symmetry and internal  
20 inhomogeneity.

### 21 *3.3 Two-dimensional distribution of the quantized DD's opacity*

22 2D grid boxes shown in Fig. 5 describe the more detailed 2D spatial distributions of



1 the opacity values. Each grid box with a unique averaged opacity value corresponds to  
2 a specific dust concentration. The 2D distribution image reflects the basic features of  
3 inhomogeneity and quasi-symmetry inside the DD. The grids used to quantify spatial  
4 distribution of opacity values are able to present the similar spatial variability like grid  
5 boxes defined in DD numerical models to simulate spatial distribution of physical  
6 properties(Mason et al., 2013;Gu et al., 2006).

7 The opacity is related to the PM's concentration, composition, and size distribution  
8 in DDs (Metzger et al., 1999). The value of the opacity is assumed to decrease with  
9 increasing height due to gravity that prevents larger particles from traveling to the  
10 upper parts of the DD. Therefore, it is expected that smaller particles could be  
11 transmitted to a higher altitud(Gu et al., 2003;Gu et al., 2007). A distinct vertical  
12 opacity gradient develops with small values at the center portion of the DD. It  
13 suggests that airflow inside DD is relatively stable and vertical mixing is weak. At the  
14 same time larger particles are transported into the outer spiral dust bands where the  
15 mixing is much stronger because of entrainment. In addition, the large number of sand  
16 vortexes at lower portions of spiral bands explains the coexistence of descending  
17 larger particles and ascending fine particles. And these results are consistent with  
18 those from numerical simulations by Gu (2007) and Gierasch (1973; 1974).

### 19 *3.4 The DD eye and the three dimensional distribution of opacity*

20 Previous research have clarified the principal characteristics of DDs that the centers  
21 of DDs have low pressure, weak airflow, and almost zero tangential velocity (Fiedler  
22 and Kanak, 2001;Kanak, 2006). Dust concentration in this inner core region is much



1 lower compared to other portion of DD (Balme and Greeley, 2006;Gu et al., 2003). It  
2 is similar to the eye of hurricanes or typhoons characterized by light wind, clear skies.  
3 Though the DD's eye is difficult to observe directly, the variation of opacity with a  
4 bimodal distribution at the same height ( Fig.4) indicates that the DD's eye does exist.  
5 Fig. 6 illustrates a conceptual mode of the horizontal cross section of a DD. The DD  
6 DD's eye diameters are measured by  $2R$  and  $2r$ , respectively, The line segment FG is  
7 the distance between two peak opacity points (F and G) away from the eye, H with  
8 minimum opacity is the center of the eye. The opacity value at point A in Fig. 6, for  
9 instance, is the accumulated opacity through distance from B to C. The changes in  
10 opacity from B to C, however, is unknown. So, we assume the horizontal opacity  
11 values are constant between B and C.

12 A more detailed example illustrated by Fig. 4 describes the DD having a diameter  
13 of 12 m and a height of 4 m. The horizontal variation of opacity values shows an  
14 obvious bimodal distribution. The peak opacity value is located at 3 m away from the  
15 DD's centerline. Therefore, it can be determined that the outer radius of DD is 6 m  
16 and the inner radius of DD's eye is 3 m at the same height. Every segment (e.g., B to  
17 C) is divided into four equal sub-segments, and the horizontal distribution can be  
18 derived accordingly. With this method, we can obtain a 3D structure of the DD by  
19 calculating the horizontal distribution at different heights as shown in Fig. 7 (i.e., at  
20 3m, 6 m, 9 m, and 12 m). The opacity values increase first and then decreases from  
21 the center to both sides of the DD that make up the bimodal distribution. The 3D  
22 structure of DD as described in Fig. 7 represents the fundamental features of



1 inhomogeneity and quasi-symmetric opacity distribution.

2 The results demonstrate that the methodology to derive the 3D opacity structure in  
3 a DD is feasible and practicable. The future effort to improve this methodology is to  
4 identify and quantify discrepancies between the assumed opacity values and observed  
5 ones from B to C. It can be realized using more than one camera to provide digital  
6 images of the same DD from different angles. The more precise and accurate 3D  
7 structure of DD will be obtained with the improved measurements.

8

#### 9 **4 Summary and Conclusions**

10 This study is the first to apply Digital Optical Method (DOM) to quantify the  
11 opacity of dust devils (DDs) in the Taklimakan Desert. The two dimensional (2D)  
12 distribution of opacity values inside the DD was obtained by DOM and correspondent  
13 observational data analysis. Analysis results show that the opacity values of DDs  
14 decrease monotonically with height; the opacity decreases more significantly at lower  
15 levels than upper ones. Also, the averaged lapse rate for the profile is 4.1% below 10  
16 m height over which the lapse rate drops to 0.6%. The horizontal opacity values from  
17 the DD's eye to both edges of the DD increases, reaches a peak value, and then  
18 diminishes rapidly. The quasi-asymmetry distribution of dust particles inside DDs can  
19 be characterized by the bimodal distribution from observed opacity values from the  
20 DD's eye to the outward horizontal directions. The distinct horizontal distribution of  
21 opacity values proves the existence of the DD's eye which is difficult to be observed  
22 directly. A typical 3D structure of opacities is developed based on the assumption of



1 constant opacity through horizontal cross-sections of a DD. Such results are  
2 encouraging and support the use of DOM as alternative to other instrumentally  
3 intensive, generally expensive methodologies for DD observations.

#### 4 **5 Prospect**

5 In order to improve the quality of DD observations using DOM, the following key  
6 issues will be addressed: 1) the proportionality coefficient ( $K$ ) is not available so far  
7 for desert dust devils. The  $K$  value we used in our opacity calculations is for white  
8 plume (light scattering plume) whose optical properties is definitely different from  
9 DD (desert dust particles), the estimate of  $K$  for desert dust is identified as a urgent  
10 need for our future study; 2) a scaling model of DD size from DD images is required  
11 if there is no reference to determine DD scale; 3) the results documented in this study  
12 are far from generalized characteristics of DD opacity. In order to realize statistical  
13 analysis of large sized samples, more observations including carefully-designed  
14 specific field campaigns are needed for characterizing DD opacities; 4) the validation  
15 of calculated opacities inside DD column is also a challenge for us. It is essential to  
16 collect other independent observation data of DD for this purpose.

17 A new method to convert 2D structure of opacity using multiple-camera digital  
18 optical method (MDOM) to 3D will be developed. The results from further improved  
19 MDOM will be related to the estimate of vertical gradient of dust concentration. In  
20 addition, the wind shear and Reynolds stress will be considered in the improved  
21 system in order to realize the parameterization of vertical dust flux caused by DDs.

22 The opacity of dust devils may also be affected by meteorology like ambient wind



1 and temperature difference between surface and air. Which may influence the strength  
2 and size of dust devils. High-strength dust devils can roll up more dust particles,  
3 affecting the opacity of dust devils. So in the following study, more observation sites  
4 will be set to measure meteorology such as ambient wind, temperature difference  
5 between surface and air, wind of dust devils, temperature and pressure difference  
6 between core of dust devils and surrounding environment, etc.

7

## 8 **Acknowledgments**

9 This research was supported the National Natural Science Foundation of China  
10 (41375158; 41175093; 41405013) and the Research Starting Project of NUIST  
11 (20110304) of China. Any opinions, findings, and conclusions or recommendations  
12 expressed in this paper are those of the authors and do not necessarily reflect the view  
13 of the Nanjing University of Information Science and Technology, University of  
14 Illinois at Urban and Champaign, or any organizations and government agencies.

15

## 16 **References**

17 American Society of Testing Materials (2013) Standard Test Method for Determining  
18 the Opacity of a Plume in the Outdoor Ambient Atmosphere (ASTM D-7520),  
19 <http://www.astm.org/Standards/D7520.htm>.  
20 Balme, M., and Greeley, R.: Dust devils on Earth and Mars, *Reviews of Geophysics*,  
21 44, 2006, doi: 10.1029/2005RG000188.  
22 Bluestein, H. B., Weiss, C. C., and Pazmany, A. L.: Doppler radar observations of  
23 dust devils in Texas, *Monthly weather review*, 132, 209-224, 2004,  
24 doi: [http://dx.doi.org/10.1175/1520-0493\(2004\)132<0209:DROODD>2.0.CO;2](http://dx.doi.org/10.1175/1520-0493(2004)132<0209:DROODD>2.0.CO;2).



- 1 Duan, J.P., Han, Y. X., Zhao, T. L., and Song, H. D.: The contribution of dust devils  
2 to atmospheric dust aerosols and its relation with solar radiation. China  
3 Environmental Science, 33, 43-48,2013. (In Chinese with English abstract)
- 4 Deng, Z.Q., Han, Y.X., Bai, Z.H.,and Zhao, T.L.:Relationship between dust aerosol  
5 and solar radiation in gebi desert in North China.China Environment Science,  
6 31(11):1761-1767,2011.(In Chinese with English abstract)
- 7 Du, K., Rood, M. J., Kim, B. J., Kemme, M. R., Franek, B., and Mattison, K.:  
8 Quantification of plume opacity by digital photography, Environmental science &  
9 technology, 41, 928-935, 2007, doi: 10.1021/es061277n.
- 10 Du K., Rood, M. J., Kim, B.J., Kemme, M. R., Franek, B., and Mattison, K.:  
11 Evaluation of digital optical method to determine plume opacity during nighttime.  
12 Environmental science & technology, 43, 783-789,2009, doi: 10.1021/es800483x.
- 13 Du, K., Shi, P., Rood, M. J., Wang, K., Wang, Y., and Varma, R. M.: Digital Optical  
14 Method to quantify the visual opacity of fugitive plumes, Atmospheric Environment,  
15 77, 983-989, 2013, doi:10.1016/j.atmosenv.2013.06.017.
- 16 Fiedler, B. H., and Kanak, K. M.: Rayleigh - Bénard convection as a tool for studying  
17 dust devils, Atmospheric Science Letters, 2, 104-113, 2001,doi : 10.1006/asle.200  
18 1.0046.
- 19 Gillette, D. A., and Sinclair, P. C.: Estimation of suspension of alkaline material by  
20 dust devils in the United States, Atmospheric Environment. Part A. General Topics,  
21 24, 1135-1142, 1990, doi:10.1016/0960-1686(90)90078-2.
- 22 Gu, Z., Zhao, Y., Yu, Y., and Feng, X.: Numerical study of the formation evolution  
23 and structure of dust devil. Acta Meteorologica Sinica, 61, 751-760,2003. (In Chinese  
24 with English abstract)
- 25 Gu, Z. L., Wei, W., and Zhao, Y.Z.: An overview of surface conditions in numerical  
26 simulations of dust devils and the consequent near-surface air flow fields. Aerosol Air  
27 Qual. Res, 10, 272-281,2010, doi: 10.4209/aaqr.2009.12.0077.
- 28 Gu, Z. L., Qiu, J., Lu, L.Y., and Zhao, Y.Z.: Advances in Study of Dust Devils,  
29 Journal of Desert Research, 5, 022, 2007. (In Chinese with English abstract)
- 30 Gu, Z., Zhao, Y., Li, Y., Yu, Y., and Feng, X.: Numerical simulation of dust lifting



- 1 within dust devils-simulation of an intense vortex, *Journal of the atmospheric sciences*,  
2 63, 2630-2641, 2006, doi: <http://dx.doi.org/10.1175/JAS3748.1>.
- 3 Gu, Z., Qiu, J., Zhao, Y., and Hou, X.: Analysis on dust devil containing loess dusts  
4 of different sizes, *Aerosol Air Qual. Res.*, 8, 65-77, 2008,doi:10.4209/aaqr.200  
5 7.03.0026.
- 6 Gierasch, P., and Goody, R.: A model of a Martian great dust storm. *Journal of the*  
7 *Atmospheric Sciences*, 30, 169-179,1973,doi: <http://dx.doi.org/10.1175/1520-0469>  
8 (1973)030<0169:AMOAMG>2.0.CO;2.
- 9 Gierasch, P. J.: Martian dust storms. *Reviews of Geophysics*, 12, 730-734,1974,  
10 doi: 10.1029/RG012i004p00730.
- 11 Han, Y., Fang, X., Xi, X., Song, L., and Yang, S.: Dust storm in Asia continent and its  
12 bio-environmental effects in the North Pacific: A case study of the strongest dust  
13 event in April, 2001 in central Asia, *Chinese Science Bulletin*, 51, 723-730, 2006,doi:  
14 10.1007/s11434-006-0723-2.
- 15 Han, Y., Dai, X., Fang, X., Chen, Y., and Kang, F.: Dust aerosols: a possible  
16 accelerant for an increasingly arid climate in North China, *Journal of Arid*  
17 *Environments*, 72, 1476-1489, 2008, doi:10.1016/j.jaridenv.2008.02.017.
- 18 Ives, R. L.: Behavior of dust devils. *Bull. Amer. Meteor. Soc.*, 28, 168-174,1947.
- 19 Ito, J., Tanaka, R. and Niino, H.: Large eddy simulation of dust devils in a  
20 diurnally-evolving convective mixed layer. *Journal of the Meteorological Society of*  
21 *Japan*, 88,63-77,2010,doi:10.2151/jmsj.2010-105.
- 22 Kanak, K. M., Lilly, D. K., and Snow, J. T.: The formation of vertical vortices in the  
23 convective boundary layer, *Quarterly Journal of the Royal Meteorological Society*,  
24 126, 2789-2810, 2000,doi: 10.1002/qj.49712656910.
- 25 Kanak, K. M.: Numerical simulation of dust devil-scale vortices, *Quarterly Journal of*  
26 *the Royal Meteorological Society*, 131, 1271-1292, 2005,doi: 10.1256/qj.03.172.
- 27 Kanak, K. M.: On the numerical simulation of dust devil-like vortices in terrestrial  
28 and Martian convective boundary layers, *Geophysical research letters*, 33, 2006,  
29 doi: 10.1029/2006GL026207.
- 30 Koch, J., and Renno, N. O.: The role of convective plumes and vortices on the global



- 1 aerosol budget, *Geophysical research letters*, 32, 2005, doi: 10.1029/2005GL023420.
- 2 Leovy, C. B.: Mars: The devil is in the dust, *Nature*, 424, 1008-1009, 2003,  
3 doi:10.1038/4241008a.
- 4 Lorenz, R.: Observing desert dust devils with a pressure logger, *Geoscientific*  
5 *Instrumentation, Methods and Data Systems*, 1, 209-220, 2012,doi:10.5194/gi-1-209  
6 -2012.
- 7 Lorenz, R. D.: Irregular dust devil pressure drops on Earth and Mars: Effect of  
8 cycloidal tracks, *Planetary and Space Science*, 76, 96-103, 2013, doi:10.1016/j.pss.20  
9 13.01.001.
- 10 Marsham, J., Parker, D., Grams, C., Johnson, B., Grey, W., and Ross, A.:  
11 Observations of mesoscale and boundary-layer scale circulations affecting dust  
12 transport and uplift over the Sahara, *Atmospheric Chemistry and Physics*, 8,  
13 6979-6993, 2008,doi:10.5194/acp-8-6979-2008.
- 14 Mason, J. P., Patel, M. R., and Lewis, S. R.: Radiative transfer modelling of dust  
15 devils, *Icarus*, 223, 1-10, 2013, doi:10.1016/j.icarus.2012.11.018.
- 16 Metzger, S. M., Carr, J. R., Johnson, J. R., Parker, T. J., and Lemmon, M. T.: Dust  
17 devil vortices seen by the Mars Pathfinder camera. *Geophysical research letters*, 26,  
18 2781-2784, 1999, doi: 10.1029/1999GL008341.
- 19 Sinclair, P. C.: Some preliminary dust devil measurements. *Monthly Weather Review*,  
20 92,1964,available at: [http://citeseerx.ist.psu.edu/viewdoc/download?doi=10.1.1.395.](http://citeseerx.ist.psu.edu/viewdoc/download?doi=10.1.1.395.3338&rep=rep1&type=pdf)  
21 [3338&rep=rep1&type=pdf](http://citeseerx.ist.psu.edu/viewdoc/download?doi=10.1.1.395.3338&rep=rep1&type=pdf).
- 22 Toigo, A. D., M. I. Richardson, S. P. Ewald, and P. J. Gierasch: Numerical simulation  
23 of Martian dust devils. *Journal of Geophysical Research: Planets* (1991–2012),  
24 108,2003, doi: 10.1029/2002JE002002.
- 25 Wei L. and Shen,Z.B.:The radiative characteristics of atmospheric dust observed from  
26 satellite.*J. Plateau Meteorology*, 17(4):347-355,1998.(In Chinese with English  
27 abstract)
- 28 Wang, M., and Zhang, R.: Frontier of atmospheric aerosols researches, *Climatic and*  
29 *Environmental Research*, 6, 119-124, 2001.( In Chinese with English abstract)
- 30 Zhang X.Y.,An, Z.S., Zhang, G.Y., Chen, T., Liu, D.S., Arimoto, R.:Transport,



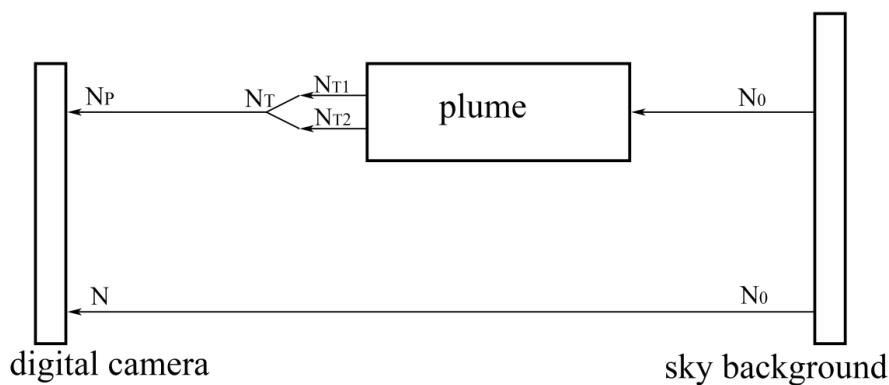
1 deposition and reflected climate change of Chinese atmospheric particulate-I. Modern  
 2 Atmospheric Aerosols, J. Science in China, 24(12):1314-1322,1994. (In Chinese with  
 3 English abstract)

4  
 5  
 6  
 7  
 8  
 9



10  
 11 **Fig.1.** A typical DD observed on July 2, 2014 (a is the original figure, b is the figure with  
 12 centerline (line 0) and guides. An upright pole near the DD as a reference for measuring the DD)

13

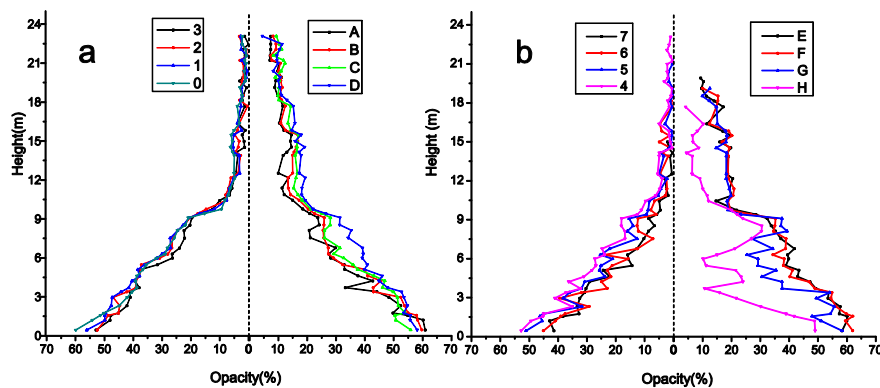


14  
 15

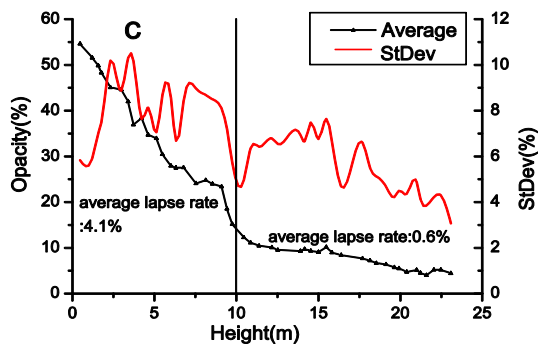
**Fig.2.** Schematic describing the transmission model to determine plume opacity



1

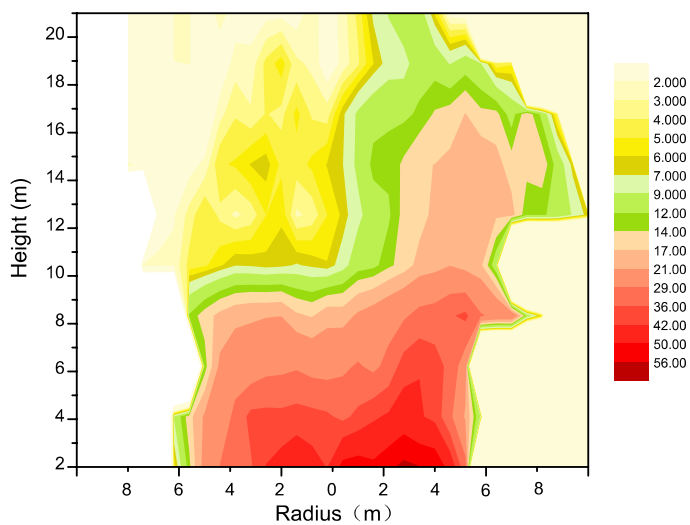


2



3

4 **Fig.3.** Vertical profiles of opacity of dust plume (a and b are the line-specific vertical profiles of  
5 opacity of dust plume, c is averaged vertical profile and vertical standard deviations of opacity of  
6 dust plume, the averaged lapse rate for the profile below 10m height is 4.1% over which it is 0.6%

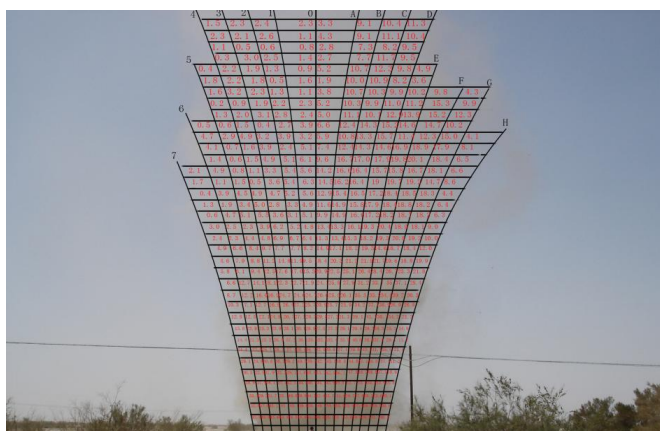


1

2

**Fig.4.**Horizontal variation of the DD's opacity(%) at different levels

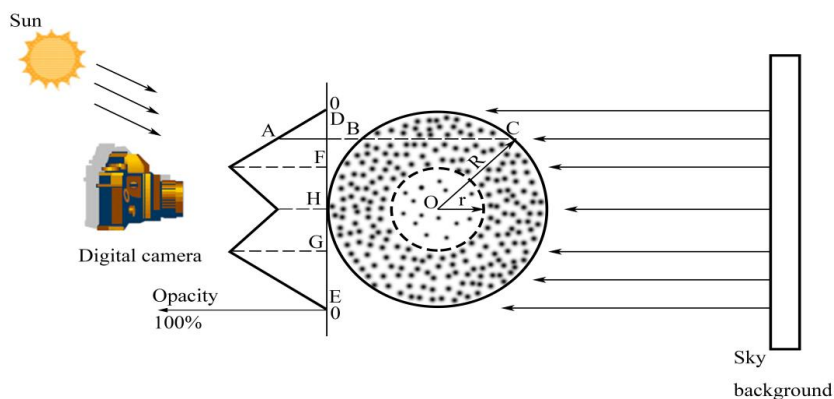
3



4

5

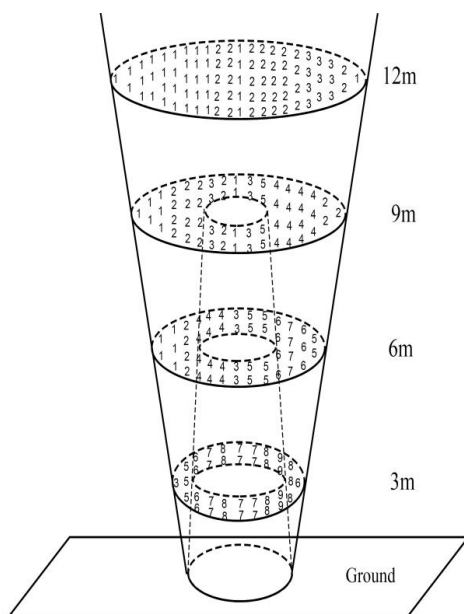
**Fig.5.** Distribution of the DD's opacity in a vertical cross section



1

2

**Fig.6.** DD's horizontal section model and the corresponding variation of opacity



3

4

**Fig.7.** 3D structure of the DD's opacity

5

6

7

8